



Cite this: *Chem. Commun.*, 2017, 53, 6621

Received 16th April 2017,
Accepted 25th May 2017

DOI: 10.1039/c7cc02918g

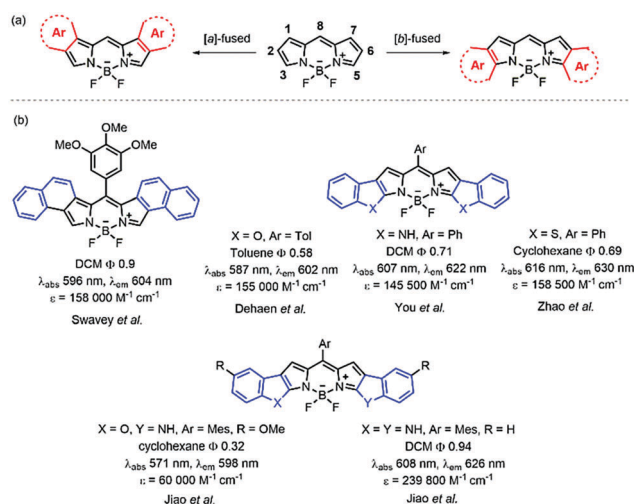
rsc.li/chemcomm

Naphtho[*b*]-fused BODIPYs: one pot Suzuki–Miyaura–Knoevenagel synthesis and photophysical properties†

Zhikuan Zhou,^{ib}*^{ab} Jianping Zhou,^a Lizhi Gai,^b Aihua Yuan^{ib}*^a and Zhen Shen*^b

Naphtho[*b*]-fused BODIPYs have been facilely synthesized via Suzuki–Miyaura–Knoevenagel reaction between mono-iodo-BODIPY or 2,6-diiodo-BODIPY with (2-formylphenyl)boronic acid. This one-pot reaction represents a very straightforward approach for tuning the absorption and emission of BODIPYs in the red visible/NIR range.

Boron dipyrromethene (BODIPY) dyes¹ have been widely used as fluorophores in fluorescent sensors,² biological labeling,³ photodynamic therapy⁴ and organic light-emitting diodes (OLEDs)⁵ due to their excellent photophysical properties, such as high photostability, sharp fluorescence emission, high fluorescence quantum yields ($\Phi_F > 0.5$) and large molar absorption coefficients. Conventional BODIPY dyes generally absorb and emit in the range of 470–530 nm. However, consideration of various practical applications of BODIPY dyes, their absorption and emission in the red visible to the near-infrared (NIR) range is more favorable. To this end, several methods have been adopted to modify the BODIPY core, such as aryl substitution at peripheral positions, substitution of a carbon atom with a nitrogen atom at the *meso* position and aromatic ring fusion.⁶ Among them, fusion with aromatic rings such as benzene, naphthalene, phenanthrene, thiophene and furan has the advantage of extending the π system and reducing the nonradiative decay through restrict rotational relaxation (Scheme 1). BODIPYs with aromatic rings fused on [*a*] and [*b*] positions are shown in Scheme 1. Aromatic [*b*]-fused BODIPYs exhibit longer red-shifted maximum absorption and emission bands compared with the [*a*]-fused mode. As shown in Scheme 1(b), indole



Scheme 1 (a) Chemical structures of [*a*]– and [*b*]–aromatic ring-fused BODIPYs. (b) Literature reported aromatic ring fused BODIPYs and their photophysical data.

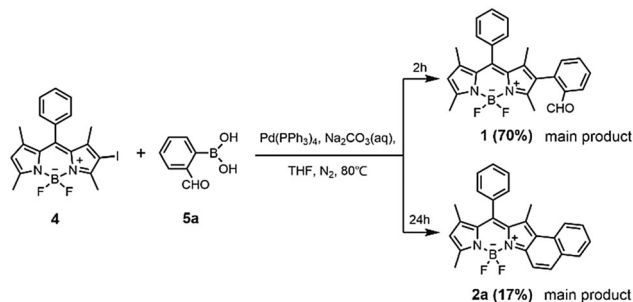
and furan ring-fused BODIPYs exhibited red-shifted absorption and emission bands and enhanced absorption coefficients upon [*b*]-annulation.⁸ The synthesis of aryl-fused BODIPYs were generally achieved *via*: (i) the condensation of aryl-fused pyrrole with an electrophilic carbonyl compound, followed by oxidation with certain oxidants and complexation with BF_3 .⁷ However, aryl-fused pyrroles were usually prepared through a multistep synthesis and the total yield was quite low. (ii) Intramolecular oxidative ring closure.⁸ In this case, two steps including palladium-catalyzed cross coupling and oxidative ring closure were required to form aromatic ring-fused BODIPYs. Herein we describe a facile synthesis and optical properties of naphtho[*b*]-fused BODIPYs *via* a one-pot Suzuki–Miyaura–Knoevenagel reaction.

Mono-iodo-BODIPY **4** was synthesized according to our previously reported procedure.⁹ Suzuki–Miyaura cross-coupling reaction of **4** and (2-formylphenyl)boronic acid **5a** was smoothly proceeded under conventional conditions (Scheme 2). The reaction, monitored by thin-layer chromatography (TLC) and UV-Vis

^a School of Environmental and Chemical Engineering, Jiangsu University of Science and Technology, Zhenjiang 212003, P. R. China. E-mail: zkzhou@just.edu.cn, aihua.yuan@just.edu.cn; Fax: +86-511-85635850; Tel: +86-511-85639001

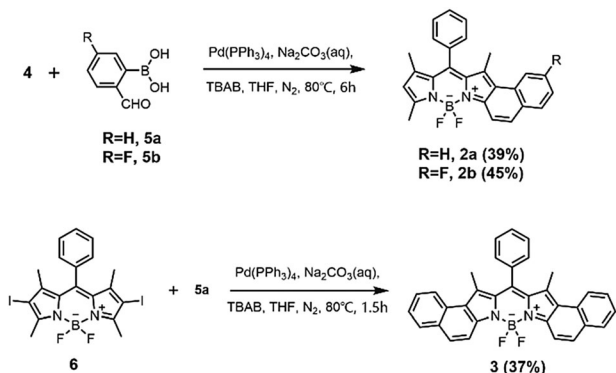
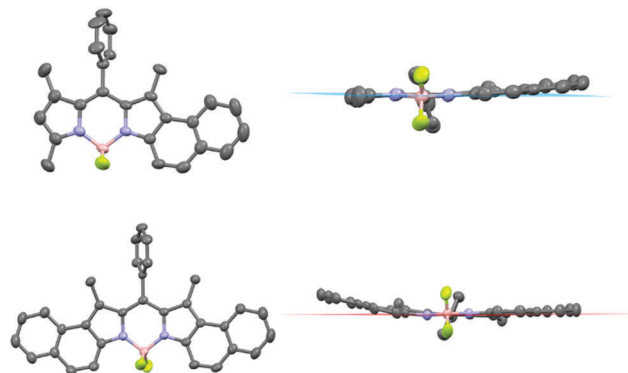
^b State Key Laboratory of Coordination Chemistry, School of Chemistry and Chemical Engineering, Nanjing University, Nanjing, 210023, P. R. China. E-mail: zshen@nju.edu.cn

† Electronic supplementary information (ESI) available: Experimental details, additional spectroscopic properties, detailed description of the computational methods and NMR spectra. CCDC 1535183 and 1535184. For ESI and crystallographic data in CIF or other electronic format see DOI: 10.1039/c7cc02918g

Scheme 2 Synthesis of mono naphtho[*b*]-fused BODIPY.

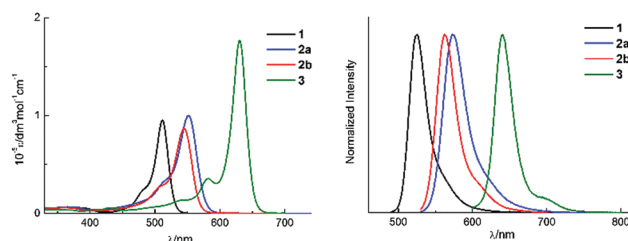
spectroscopy, was found to be complete in 2 h, affording the desired BODIPY **1** in 70% yield. Interestingly, when the cross-coupling reaction time was extended to 24 h, BODIPY **1** underwent an intramolecular Knoevenagel type condensation between the methyl group at the 3-position and the formyl group on the adjacent phenyl ring, which gave asymmetric naphthalene-fused BODIPY **2a** as the main product with an isolated yield of 17%. No other obvious colored product was found using TLC. BODIPYs **1** and **2a** were characterized by HR-MS and ^1H NMR spectroscopy. Inspired by the phase transfer catalytic feature of tetrabutylammonium bromide (TBAB) in intermolecular Aldol–Suzuki–Aldol reactions,¹⁰ we introduced it into this reaction system. It was found that after the addition of one equivalent of TBAB, the reaction of **4** and **5a** completed in 6 h and the isolated yield of **2a** was increased two times to 39% (Scheme 3). Under these one pot Suzuki–Miyaura–Knoevenagel conditions, the reaction can be complete within 1.5 h and successfully provided symmetric bis-naphtho[*b*]-fused BODIPY **3** in 35% yield (Scheme 3). Longer reaction time led to the lower yield and the decomposition of **3**, which was confirmed from the TLC and UV-Vis spectra monitoring.

Single crystals of **2a** and **3** were obtained by slow diffusion of hexane into CH_2Cl_2 solutions at room temperature. As shown in Fig. 1, both of the molecules exhibit certain distortion from planarity. The torsion angles between the *meso*-phenyl group and the indacene plane are 74.0° and 67.5° for **2a** and **3**, respectively. The dihedral angle between the fused-benzo ring and the indacene plane in BODIPY **2a** is 7.5° . BODIPY **3** displays a butterfly-like conformation, and the dihedral angle between the two planar fused naphthalene “wings” is 14.5° .

Scheme 3 Synthesis of mono and bis-naphtho[*b*]-fused BODIPY dyes.Fig. 1 X-ray crystal structures of **2a** (top) and **3** (bottom): top view (left) and side view (right). Hydrogen atoms were omitted for clarity in both views. The thermal ellipsoids were set at 50% probability.

This is quite different from the planar conformation in the bis-benzothieno[*b*]-fused and biphenyl-fused BODIPYs (Scheme 1).^{8b,f}

The absorption and emission spectra of the dyes in CH_2Cl_2 solution are shown in Fig. 2 and the main photophysical data are summarized in Table 1. Details of the main spectral bands of the electronic absorption and fluorescence emission spectra and the steady-state and time-resolved fluorescence spectroscopy properties in hexane, toluene, dichloromethane, THF, acetonitrile and methanol are summarized in Table S1, ESI.† The absorption and emission band of mono-naphtho[*b*]-fused **2a** red-shifted by 41 nm relative to the classic BODIPY **1**. Upon further naphtho[*b*]-fusion to form **3**, which has two naphthalene rings fused on both pyrrole moieties, a 78 nm red shift occurs with a peak centered at 630 nm and a large molar absorption coefficient ($\epsilon = 175\,660\ \text{M}^{-1}\ \text{cm}^{-1}$), indicating an efficient π -extension effect induced by a fused naphthalene group on the [*b*] position.¹¹ When

Fig. 2 Overlaid UV/Vis absorption (left) and normalized fluorescence (right) spectra of **1**, **2a**, **2b** and **3** in CH_2Cl_2 .Table 1 Spectroscopic data of **1**, **2a**, **2b** and **3** in CH_2Cl_2

	λ_{abs} [nm]	ϵ_{abs}^a [$\text{mol}^{-1}\ \text{cm}^{-1}\ \text{L}$]	λ_{em} [nm]	$\Delta\nu_{\text{abs-em}}^b$ [cm^{-1}]	Φ_{F}^c	τ_{f}^d [ns]
1	511	95 200	525	522	0.82	4.02
2a	552	100 000	573	664	0.30	3.70
2b	545	86 400	562	555	0.37	2.80
3	630	175 660	640	248	0.06	3.29

^a Molar absorption coefficients measured in solutions containing 1% THF as a co-solvent. ^b Stokes-shift value. ^c Fluorescence quantum yields were calculated using rhodamine 6G as the standard ($\Phi_{\text{F}} = 0.95$ in ethanol) for **1**, **2a** and **2b** and zinc phthalocyanine as the standard ($\Phi_{\text{F}} = 0.45$ in PrOH) for **3** and the standard errors are less than 5%. ^d Half-life period.

an electron withdrawing group is introduced at the naphthalene ring to form **2b**, the main spectral band is 7 nm blue shifted relative to the spectrum of **2a**. The observed absorption maxima of naphtho[*b*]-fused BODIPY dyes do not show a clear variation trend as a function of polarity of the solvents. A similar trend is observed in the emission band. Naphtho[*b*]-fusion on the BODIPY core leads to the decrease of fluorescence quantum yields of **2a** (0.30) and **3** (0.06) due to an increase in the nonradiative deactivation rate constant (Table 1). It is well known that one of the main drawbacks of red-emitting dyes is their lower fluorescence quantum yield, since the ground and excited states are energetically closer, and the probability of internal conversion is greatly enhanced due to the increased likelihood of vibrational coupling between the electronic excited and ground states.⁹ The fluorescence decay profiles could be described with a single-exponential fit with fluorescence lifetimes in the 2.59–4.35 ns range for all the solvents investigated. As expected, the non-radiative decay constants of **3** are very large and significantly higher than that of non-fused BODIPY **1** (Table S1, ESI†).

In order to gain in-depth insight into the relationship between aryl-fused structures and electronic structures, and optoelectronic properties, theoretical calculations were performed for BODIPYs **1–3** using the time-dependent density functional theory (TDDFT) method at the B3LYP/6-31G(d) level.¹² Partial MO energy diagrams of **1–3** are shown in Fig. 3, while the calculated transition energies, oscillator strengths (f), and configurations are summarized in Table 2. The phenyl substitutions at *meso*-positions of all compounds and at 2-position of **1** are nearly perpendicular to the BODIPY skeleton, on which the HOMO and the LUMO are fully delocalized (Fig. 3). Based on the TDDFT calculations, the main absorption bands of these dyes are attributed to transitions from the HOMO to the LUMO. The second lowest-energy band of 474 nm ($f = 0.77$) for dye **2a** mainly contributed to the absorption peak, because the oscillator strength of the calculation S_1 state is almost zero. For BODIPY **3**, the higher energy shoulder band at around 580 nm mainly is attributed to transition from the HOMO–1 to the LUMO (Table 2). In contrast to the unfused structure **1**, BODIPYs **2a**, **2b** and **3** with fused rings exhibit a narrow HOMO–LUMO gap.

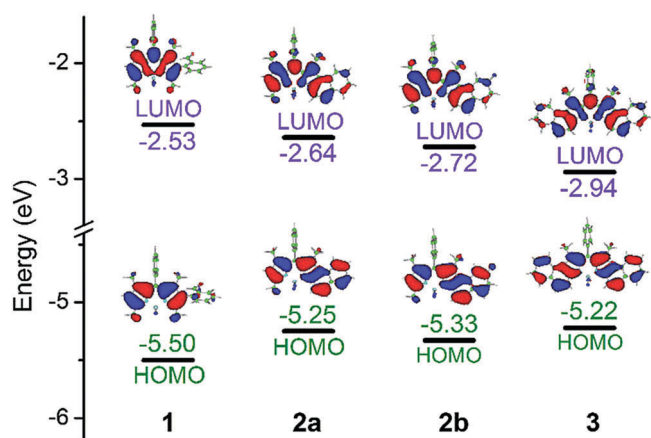


Fig. 3 The energy level diagrams of the frontier π -MOs of **1–3** using the B3LYP functional with 6-31G(d) basis sets. The angular nodal patterns are shown at an isosurface value of 0.02 a.u.

Table 2 Selected transition energies and wave functions of **1**, **2a**, **2b**, and **3** calculated using the TDDFT method (B3LYP/6-31G(d))

Compd.	Energy [nm]	f^a	Orbitals ^b (coefficient)
1	425	0.54	H → L (88%), H–1 → L (12%)
2a	493	0.01	H–1 → L (97%)
	474	0.77	H → L (96%)
2b	494	0.17	H–1 → L (62%), H → L (38%)
	467	0.59	H → L (60%), H–1 → L (37%)
3	547	0.21	H–1 → L (73%), H → L (26%)
	532	0.97	H → L (74%), H–1 → L (26%)

^a Oscillator strength. ^b MOs involved in the transitions with H and L denoting the HOMO and the LUMO, respectively.

The large MO coefficients on the peripheral fused rings account for the destabilization of the HOMO, while the smaller MO coefficients in the context of the LUMO along with the large MO coefficients at the points of attachment to the BODIPY core account for the stabilization of the LUMO. This indicates that the fused rings effectively extend the π -systems. The mono- and bis-naphthalene-fused BODIPYs **2a** and **3** show nearly identical HOMO energies; however, the LUMO energy of **3** was significantly stabilized, resulting in a red shift of the main absorption band relative to that of **2a**.

In conclusion, BODIPYs with one and two naphthalene rings fused at the *b* position have been synthesized from iodo-substituted BODIPYs and (2-formylphenyl)boronic acid through Suzuki–Miyaura–Knoevenagel one pot reaction with moderate yields. BODIPYs **2** and **3** represent the first examples of naphtho[*b*]-fused BODIPYs. The fusion of the naphthalene ring greatly extends the π -conjugation of BODIPY **3** and thus made it exhibit NIR absorption. Theoretical calculations suggest that naphthalene-fused BODIPYs display markedly stabilized LUMO energy, which can be used in the field of optoelectronics such as electron transport materials. The methyl group at the 5-position of the asymmetric dye **2** can be further modified with the analyte-active group to fabricate novel NIR chemosensors.

We acknowledge financial support provided by the National Natural Science Foundation of China (21501073) to Z. Z., (51672114) to A. Y. and (21371090) to Z. S. Theoretical calculations were carried out at the High-Performance Computing Center in Nanjing University.

Notes and references

‡ Crystallographic data for **2a**: $C_{26}H_{21}BF_2N_2$, $M_w = 410.26$, monoclinic, space group $C2/c$, $a = 21.110(8)$, $b = 10.940(4)$, $c = 20.341(12)$ Å, $\alpha = 90.00^\circ$, $\beta = 118.052(3)^\circ$, $\gamma = 90.00^\circ$, $V = 4146(3)$ Å³, $Z = 8$, $\rho_{\text{calcd}} = 1.377$ g cm⁻³, $T = 23(2)$ °C, 4783 measured reflections, 3162 unique reflections ($R_{\text{int}} = 0.0460$), $R = 0.0772$ ($I > 2s(I)$), $R_w = 0.2344$ (all data), goodness-of-fit on $|F|^2 = 1.020$, CCDC 1535183. † Crystallographic data for **3**: $C_{33}H_{23}BF_2N_2$, $M_w = 496.34$, monoclinic, space group $C2/c$, $a = 16.140(5)$, $b = 14.391(4)$, $c = 21.159(6)$ Å, $\alpha = 90.00^\circ$, $\beta = 103.057(3)^\circ$, $\gamma = 90.00^\circ$, $V = 4787(2)$ Å³, $Z = 8$, $\rho_{\text{calcd}} = 1.377$ g cm⁻³, $T = 23(2)$ °C, 5564 measured reflections, 3792 unique reflections ($R_{\text{int}} = 0.0411$), $R = 0.0878$ ($I > 2s(I)$), $R_w = 0.2539$ (all data), goodness-of-fit on $|F|^2 = 1.155$, CCDC 1535184. ‡

- (a) G. Ulrich, R. Ziessel and A. Harriman, *Angew. Chem., Int. Ed.*, 2008, **47**, 1184–1201; (b) A. Loudet and K. Burgess, *Chem. Rev.*, 2007, **107**, 4891–4932; (c) R. Ziessel, G. Ulrich and A. Harriman, *New J. Chem.*, 2007, **31**, 496–501.
- (a) S. Wang, H. Liu, J. Mack, J. Tian, B. Zou, H. Lu, Z. Li, J. Jiang and Z. Shen, *Chem. Commun.*, 2015, **51**, 13389–13392; (b) Y. Ni and J. Wu,

- Org. Biomol. Chem.*, 2014, **12**, 3774–3791; (c) Z. Liu, W. He and Z. Guo, *Chem. Soc. Rev.*, 2013, **42**, 1568–1600; (d) X. Qu, C. Li, H. Chen, J. Mack, Z. Guo and Z. Shen, *Chem. Commun.*, 2013, **49**, 7510–7512; (e) N. Boens, V. Leen and W. Dehaen, *Chem. Soc. Rev.*, 2012, **41**, 1130–1172.
- 3 (a) A. Fernandez and M. Vendrell, *Chem. Soc. Rev.*, 2016, **45**, 1182–1196; (b) T. Kowada, H. Maeda and K. Kikuchi, *Chem. Soc. Rev.*, 2015, **44**, 4953–4972; (c) Z. Guo, S. Park, J. Yoon and I. Shin, *Chem. Soc. Rev.*, 2014, **43**, 16–29.
- 4 (a) J. Tian, J. Zhou, Z. Shen, L. Ding, J.-S. Yu and H. Ju, *Chem. Sci.*, 2015, **6**, 5969–5977; (b) A. Kamkaew, S. H. Lim, H. B. Lee, L. V. Kiew, L. Y. Chung and K. Burgess, *Chem. Soc. Rev.*, 2013, **42**, 77–88; (c) Y. Yang, Q. Guo, H. Chen, Z. Zhou, Z. Guo and Z. Shen, *Chem. Commun.*, 2013, **49**, 3940–3942.
- 5 (a) Q. Liu, X. Wang, H. Yan, Y. Wu, Z. Li, S. Gong, P. Liu and Z. Liu, *J. Mater. Chem. C*, 2015, **3**, 2953–2959; (b) H. Liu, H. Lu, Z. Zhou, S. Shimizu, Z. Li, N. Kobayashi and Z. Shen, *Chem. Commun.*, 2015, **51**, 1713–1716; (c) C.-L. Liu, Y. Chen, D. P. Shelar, C. Li, G. Cheng and W.-F. Fu, *J. Mater. Chem. C*, 2014, **2**, 5471–5478.
- 6 H. Lu, J. Mack, Y. Yang and Z. Shen, *Chem. Soc. Rev.*, 2014, **43**, 4778–4823.
- 7 (a) S. Swavey, M. Coladipietro, A. Burbayea and J. A. Krause, *Eur. J. Org. Chem.*, 2016, 4429–4435; (b) A. Bessette, T. Auvray, D. Desilets and G. S. Hanan, *Dalton Trans.*, 2016, **45**, 7589–7604; (c) J. Wang, Q. Wu, Y. Xu, C. Yu, Y. Wei, X. Mu, E. Hao and L. Jiao, *RSC Adv.*, 2016, **6**, 52180–52188; (d) C. Maeda, T. Todaka and T. Ema, *Org. Lett.*, 2015, **17**, 3090–3093; (e) A. Wakamiya, T. Murakami and S. Yamaguchi, *Chem. Sci.*, 2013, **4**, 1002–1007; (f) Y. Ni, W. Zeng, K.-W. Huang and J. Wu, *Chem. Commun.*, 2013, **49**, 1217–1219; (g) S. G. Awuah, J. Polreis, V. Biradar and Y. You, *Org. Lett.*, 2011, **13**, 3884–3887; (h) A. B. Descalzo, H.-J. Xu, Z.-L. Xue, K. Hoffmann, Z. Shen, M. G. Weller, X.-Z. You and K. Rurack, *Org. Lett.*, 2008, **10**, 1581–1584; (i) Z. Shen, H. Röhr, K. Rurack, H. Uno, M. Spieles, B. Schulz, G. Reck and N. Ono, *Chem. – Eur. J.*, 2004, **10**, 4853–4871; (j) J. Chen, A. Burghart, A. Derecskei-Kovacs and K. Burgess, *J. Org. Chem.*, 2000, **65**, 2900–2906.
- 8 (a) Y. Gobo, M. Yamamura, T. Nakamura and T. Nabeshima, *Org. Lett.*, 2016, **18**, 2719–2721; (b) Z.-B. Sun, M. Guo and C.-H. Zhao, *J. Org. Chem.*, 2016, **81**, 229–237; (c) Y. Ni, R. K. Kannadorai, J. Peng, S. W. K. Yu, Y.-T. Chang and J. Wu, *Chem. Commun.*, 2016, **52**, 11504–11507; (d) J. Wang, J. Li, N. Chen, Y. Wu, E. Hao, Y. Wei, X. Mu and L. Jiao, *New J. Chem.*, 2016, **40**, 5966–5975; (e) X. Zhou, Q. Wu, Y. Feng, Y. Yu, C. Yu, E. Hao, Y. Wei, X. Mu and L. Jiao, *Chem. – Asian J.*, 2015, **10**, 1979–1986; (f) Y. Wu, C. Cheng, L. Jiao, C. Yu, S. Wang, Y. Wei, X. Mu and E. Hao, *Org. Lett.*, 2014, **16**, 748–751; (g) L. Luo, D. Wu, W. Li, S. Zhang, Y. Ma, S. Yan and J. You, *Org. Lett.*, 2014, **16**, 6080–6083; (h) E. Heyer, P. Retailleau and R. Ziessel, *Org. Lett.*, 2014, **16**, 2330–2333; (i) Y. Hayashi, N. Obata, M. Tamaru, S. Yamaguchi, Y. Matsuo, A. Saeki, S. Seki, Y. Kureishi, S. Saito, S. Yamaguchi and H. Shinokubo, *Org. Lett.*, 2012, **14**, 866–869.
- 9 H. Lu, Q. Wang, L. Gai, Z. Li, Y. Deng, X. Xiao, G. Lai and Z. Shen, *Chem. – Eur. J.*, 2012, **18**, 7852–7861.
- 10 R. Kumar, Richa, N. H. Andhare, A. Shard and A. K. Sinha, *Chem. – Eur. J.*, 2013, **19**, 14798–14803.
- 11 V. Leen, W. Qin, W. Yang, J. Cui, C. Xu, X. Tang, W. Liu, K. Robeyns, L. Van Meervelt, D. Beljonne, R. Lazzaroni, C. Tonnelé, N. Boens and W. Dehaen, *Chem. – Asian J.*, 2010, **5**, 2016–2026.
- 12 M. J. Frisch, *et al.*, *Gaussian 09, Revision B.01*, Gaussian, Inc., Wallingford, CT, 2009. See the ESI† for the full list of authors.